plants

MDPI

Article

A Rapid Method for Detecting Normal or Modified Plant and Algal Carbonic Anhydrase Activity Using *Saccharomyces cerevisiae*

Ashwani K. Rai [1], Robert J. DiMario [2], Remmy W. Kasili [1], Michael Groszmann [3], Asaph B. Cousins [2], David Donze [1] and James V. Moroney [1,*]

[1] Department of Biological Sciences, Louisiana State University, Baton Rouge, LA 70803, USA; arai5@lsu.edu (A.K.R.); rkasili@lsu.edu (R.W.K.); ddonze@lsu.edu (D.D.)
[2] School of Biological Sciences, Washington State University, Pullman, WA 99164, USA; robert.dimario@wsu.edu (R.J.D.); acousins@wsu.edu (A.B.C.)
[3] ARC Centre of Excellence in Translational Photosynthesis, Research School of Biology, Australian National University, Linnaeus Building, 134 Linnaeus Way, Canberra, ACT 2601, Australia; michael.groszmann@anu.edu.au
* Correspondence: btmoro@lsu.edu

Abstract: In recent years, researchers have attempted to improve photosynthesis by introducing components from cyanobacterial and algal CO_2-concentrating mechanisms (CCMs) into terrestrial C_3 plants. For these attempts to succeed, we need to understand the CCM components in more detail, especially carbonic anhydrase (CA) and bicarbonate (HCO_3^-) transporters. Heterologous complementation systems capable of detecting carbonic anhydrase activity (i.e., catalysis of the pH-dependent interconversion between CO_2 and HCO_3^-) or active HCO_3^- transport can be of great value in the process of introducing CCM components into terrestrial C_3 plants. In this study, we generated a *Saccharomyces cerevisiae* CA knock-out (Δ*NCE103* or Δ*CA)* that has a high-CO_2-dependent phenotype (5% (*v*/*v*) CO_2 in air). CAs produce HCO_3^- for anaplerotic pathways in *S. cerevisiae*; therefore, the unavailability of HCO_3^- for neutral lipid biosynthesis is a limitation for the growth of Δ*CA* in ambient levels of CO_2 (0.04% (*v*/*v*) CO_2 in air). Δ*CA* can be complemented for growth at ambient levels of CO_2 by expressing a CA from human red blood cells. Δ*CA* was also successfully complemented for growth at ambient levels of CO_2 through the expression of CAs from *Chlamydomonas reinhardtii* and *Arabidopsis thaliana*. The Δ*CA* strain is also useful for investigating the activity of modified CAs, allowing for quick screening of modified CAs before putting them into the plants. CA activity in the complemented Δ*CA* strains can be probed using the Wilbur–Anderson assay and by isotope exchange membrane-inlet mass spectrometry (MIMS). Other potential uses for this new Δ*CA*-based screening system are also discussed.

Keywords: carbonic anhydrase; CA activity; C_3 plants; *S. cerevisiae*; Arabidopsis; protein expression; photosynthesis; MIMS

Citation: Rai, A.K.; DiMario, R.J.; Kasili, R.W.; Groszmann, M.; Cousins, A.B.; Donze, D.; Moroney, J.V. A Rapid Method for Detecting Normal or Modified Plant and Algal Carbonic Anhydrase Activity Using *Saccharomyces cerevisiae*. *Plants* **2022**, *11*, 1882. https://doi.org/10.3390/plants11141882

Academic Editors: Natalia N. Rudenko and Vasily V. Terentyev

Received: 15 June 2022
Accepted: 7 July 2022
Published: 20 July 2022

1. Introduction

Carbonic anhydrases (CAs) catalyze the interconversion between CO_2 and bicarbonate (HCO_3^-) in solutions [1]. Although the interconversion of CO_2 and HCO_3^- happens without a CA, it occurs at a very slow rate. CAs are essential for organisms to ensure they have a quick supply of CO_2 and HCO_3^- for various metabolic pathways. CAs also play a crucial role in photosynthesis. For example, the CO_2-concentrating mechanisms (CCMs) of *Chlamydomonas reinhardtii* and cyanobacteria are powered by CAs [2–5]. In the biophysical CCMs of cyanobacteria and green algae, ribulose 1,5-bisphosphate carboxylase/oxygenase (Rubisco) is packaged in very specific compartments—carboxysomes for cyanobacteria and pyrenoids for green algae. The CCMs work to accumulate HCO_3^- to high levels in

the cytosol (cyanobacteria) or chloroplast stroma (eukaryotic algae); then a specific CA is needed to convert the HCO_3^- to CO_2 for photosynthesis. This creates a local environment around Rubisco that has an elevated CO_2 concentration. In *C. reinhardtii*, the conversion of HCO_3^- to CO_2 is catalyzed by CAH3 in the thylakoid lumen inside the pyrenoid. Loss of this thylakoid CAH3 in *C. reinhardtii* results in very slow growth rates at ambient levels of CO_2 (~0.04% (v/v) CO_2 in air) [6]. Similarly, carboxysomal CAs in cyanobacteria are required for the conversion of accumulated HCO_3^- to CO_2 for fixation by Rubisco [7]. For photosynthetic organisms to function efficiently, the CAs must be in the correct inter- and intracellular locations. For example, cyanobacterial CAs inside the carboxysomes are critical for maintaining the CCM, but CA activity in the cytoplasm disrupts the CCM. Price et al. [8] showed that CA expression in the cytoplasm of *Synechocystis* cells caused the CCM to short-circuit.

In C_4 plants, the CCM is maintained by CA activity in mesophyll cells [9]. For C_4 plants, the first step of photosynthesis is the conversion of CO_2 that diffuses into the leaf mesophyll cells to HCO_3^-, which is catalyzed by a cytosolic CA [9]. DiMario et al. [10] demonstrated that the elimination of mesophyll cytoplasmic CA activity causes a reduction in photosynthesis for C_4 plants grown in ambient levels of CO_2. C_3 plants, in contrast, do not have a CCM. However, C_3 plants still have a large number of genes encoding CA. In Arabidopsis, the α, β, γ, and γ-like isoforms of CA are encoded by 17 distinct genes [2]. The role of CAs in terrestrial C_3 plants is not well understood due to the compensatory effect of multiple isoforms. For example, DiMario, et al. [11] investigated the effects of knocking out the Arabidopsis CAs βCA2 and βCA4, which are present in the cytosol of leaf mesophyll cells, and observed that eliminating only one of the CAs resulted in no observable phenotype. When both βCA2 and βCA4 were knocked out, plants were unable to grow normally in low-CO_2 conditions. In addition, Medina-Puche et al. [12] and Hines et al. [13] observed that single knock-out lines for most βCAs in Arabidopsis had normal growth on air.

There have been attempts in recent years to improve photosynthesis by introducing CCM components from cyanobacteria, algae, or C_4 plants into terrestrial C_3 plants [14–16]. For these approaches to work, CAs must be modified and retargeted to specific locations in C_3 plants. This requires targeting CAs to the chloroplast thylakoid lumen or the cell wall. The CAs need to be modified and tagged to determine whether they are being targeted to the correct intracellular location. Thus, a rapid screen is needed to determine whether a protein modification inhibits CA activity. Transforming prospective CAs into plants is possible but requires significant time and resources. Heterologous complementation systems capable of detecting CA activity or active bicarbonate transport are valuable when studying CCM components in order to transform them into plants.

Here, we determined whether the high-CO_2-dependent *Saccharomyces cerevisiae* CA knock-out line, Δ*NCE103* (referred to here as Δ*CA*), is suitable as a heterologous complementation system for the detection of active CAs from plants and algae. The Δ*CA* strain cannot grow on ambient levels of CO_2 but can grow on high levels of CO_2 (5% CO_2 (v/v) in the air). The Δ*CA* strain lacks the gene *NCE103*, which encodes a single native *S. cerevisiae* CA [17]. It has been proposed that the loss of this native CA results in *S. cerevisiae* cells that do not have enough HCO_3^- for important metabolic processes such as fatty acid and nucleotide synthesis [18]. It has been speculated that *S. cerevisiae* requires some CA activity for survival at ambient levels of CO_2 because the uncatalyzed rate of CO_2 hydration to HCO_3^- produces insufficient HCO_3^- for anaplerotic pathways [19,20].

Aguilera et al. [18] hypothesized that Δ*CA* is not viable in ambient CO_2 largely because the cellular HCO_3^- level was insufficient for generating lipids. *S. cerevisiae* uses acetyl-CoA as a building block to synthesize neutral lipids (NL) such as triglycerides (TGs) and sterol-esters (SEs) [21]. The first step in fatty acid biosynthesis is the carboxylation of acetyl-CoA to malonyl-CoA [22]. This reaction uses HCO_3^- generated from CO_2 by the native CA in the wild-type *S. cerevisiae* cell.

Therefore, Δ*CA* can be used to detect and analyze the activity of normal or modified CAs and unusual CA-like proteins. To test this Δ*CA*-based complementation system, we first used Δ*CA* to investigate the activity of the human CA II (hCA) protein. We then tested the viability of tagged and codon-optimized hCA proteins to see if CA activity is affected by such modifications. We also tested the activity of CAs located in the mitochondria and thylakoids of *C. reinhardtii.* The mitochondrial CAs, CAH4 and CAH5, are β-CAs that are highly expressed in *C. reinhardtii* cells grown in ambient levels of CO_2 [23,24]. They have been shown to be necessary for optimal photosynthesis in cells grown in limiting-CO_2 conditions [25]. CAH3 is an α-CA located in the thylakoid lumen of *C. reinhardtii* that generates CO_2 for fixation by Rubisco inside the pyrenoid [26,27]. We also used an *Arabidopsis thaliana* β-CA called βCA3 to see if the Δ*CA*-based heterologous complementation system works for plant CAs. Aside from viability tests, CA activity was verified using the Wilbur–Anderson assay [28] and isotope exchange membrane-inlet mass spectrometry (MIMS). The results presented in this study suggest that the Δ*CA* strain can be used to determine the activity of CAs from different sources, as well as CAs that have been modified with tags and codon optimization.

2. Results

2.1. The S. cerevisiae Strain ΔCA Has a High-CO_2-Dependent Growth Phenotype

The CO_2 level requirement of Δ*CA* was characterized by conducting growth assays on solid media supplemented with different levels of CO_2: 5% (*v*/*v*) CO_2 in air, 1% (*v*/*v*) CO_2 in air, and ambient CO_2 (~0.04% (*v*/*v*) CO_2 in the air) (Figure 1). For these experiments, Δ*CA*-EV refers to the Δ*CA* strain transformed with an empty vector (EV) containing a selectable gene. For the positive control, Δ*CA* was transformed with a vector containing the *S. cerevisiae NCE103* gene so that it expresses the native CA (Δ*CA*-*ScCA*). Unlike the positive control, Δ*CA* only grows at 5% CO_2 and dies at 1% and ambient CO_2. These results agree with an early report by Aguilera et al. [18]. To investigate the biochemical deficiency underlying the high-CO_2-dependent phenotype of Δ*CA*, we incorporated radiolabeled ^{14}C-acetic acid into Δ*CA*-EV, Δ*CA*-*ScCA*, and Δ*CA*-*hCA*-YCO (Δ*CA* complemented with a *S. cerevisiae* codon-optimized (YCO) version of hCA) for one hour in ambient-CO_2 conditions and assayed ^{14}C incorporation into lipids using a silicone oil filtering centrifugation assay. The incorporation of radiolabeled ^{14}C in neutral lipids was higher in cells reconstituted with hCA compared to Δ*CA*-EV after one hour. Furthermore, Δ*CA*-*hCA*-YCO had twice the incorporation of ^{14}C in neutral lipids compared to Δ*CA* after one hour (Figure 2).

2.2. ΔCA Can Be Used as a Heterologous Complementation System to Detect CA Activity of Normal and Modified CAs

The CO_2 growth requirement of Δ*CA* was used to characterize the CA activity of normal and modified CAs. hCA complemented the Δ*CA* phenotype in ambient CO_2 and 1% CO_2 (Figures 3 and 4) [29]. In the liquid growth assay, we observed that Δ*CA*-*hCA*-YCO grew faster than Δ*CA*-EV in ambient CO_2. However, in both conditions, Δ*CA*-*ScCA* growth was faster compared to Δ*CA*-EV (Figure 3a,b). In the growth assay on solid media, Δ*CA*-*hCA*-YCO grew at a rate similar to Δ*CA*-*ScCA* in ambient CO_2 and 1% CO_2 (Figure 4). Next, we transformed Δ*CA* with YCO hCA and Arabidopsis codon-optimized (Atex) hCA and checked their effect on CA activity. Additionally, we added the tags AcV5 and eGFP to Δ*CA*-*hCA*-YCO and Δ*CA*-*hCA*-Atex to see if they affected the growth of the *S. cerevisiae*. The growth assays on solid media show that the modified hCA variants complemented Δ*CA* in ambient CO_2 and 1% CO_2 (Figure 5). We also compared the expression of hCA in the complemented lines by analyzing the protein's abundance via Western blots. In the strains complemented with the YCO genes (Δ*CA*-*hCA*-YCO, Δ*CA*-*hCA*-YCO AcV5, and Δ*CA*-*hCA*-YCO eGFP), hCA expression was higher compared to strains complemented with Atex genes (Δ*CA*-*hCA*-Atex, Δ*CA*-*hCA*-Atex AcV5, and Δ*CA*-*hCA*-Atex eGFP; Figure 6b). The protein expression of hCA was not affected by the addition of the AcV5 and eGFP

tags in strains complemented with the genes optimized for *S. cerevisiae* and Arabidopsis (Figures 6a,b and S2).

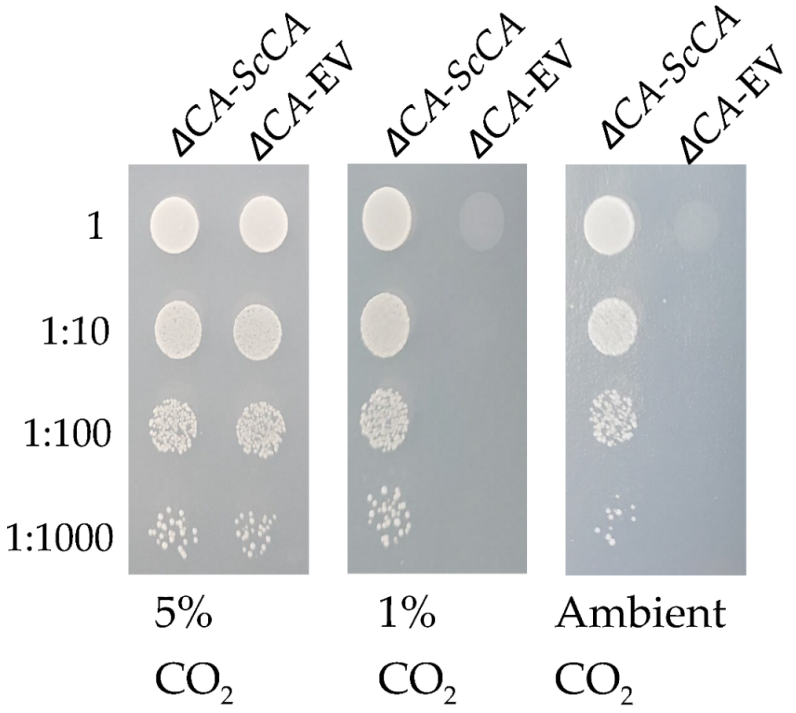

Figure 1. *S. cerevisiae* CA knock-out (Δ*CA*) cannot grow in limiting-CO_2 conditions. Δ*CA*-EV cells and *S. cerevisiae* CA knock-out out cells complemented with ScCA (Δ*CA-ScCA*) were plated in 10 µL spots on YM (-his,-trp) plates and incubated at 30 °C in 5%, 1%, and ambient (0.04%) CO_2 for 3 days. The cells were standardized to an initial OD_{600} of 0.1 and serially diluted before plating.

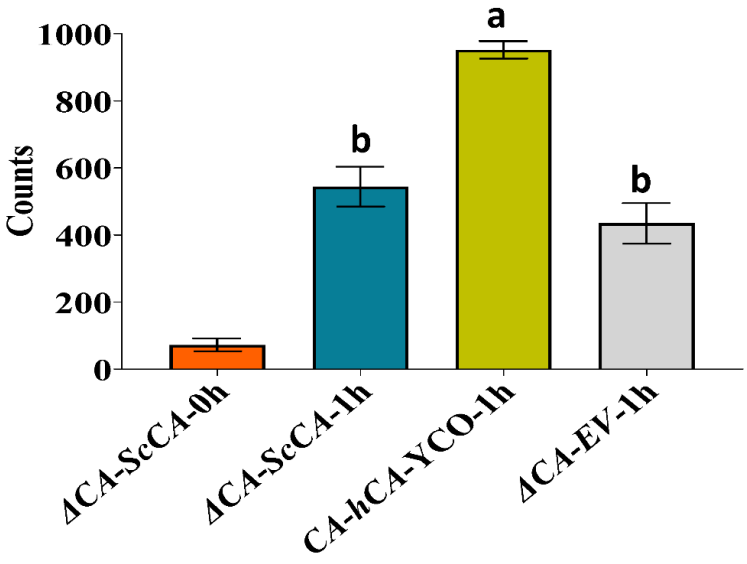

Figure 2. Δ*CA* complemented with yeast codon-optimized (YCO) human CA (*hCA*) incorporates ^{14}C-acetic acid into neutral lipids at a faster rate than Δ*CA*-EV and Δ*CA-ScCA*. Δ*CA-ScCA*, Δ*CA-hCA*-YCO, and Δ*CA*-EV cells were grown in liquid YM (-his,-trp) supplemented with ^{14}C-acetic acid for one hour in air levels of CO_2. Δ*CA-ScCA* cells supplemented with ^{14}C-acetic acid for zero hours is shown as a negative control. ^{14}C incorporation was measured using a silicone oil filtering centrifugation assay. Bars represent means, and error bars represent standard errors ($n = 3$). Statistical significance among different groups was computed with ANOVA and Tukey's post hoc HSD test ($p < 0.05$), and different statistical groups are represented by the letters a and b above bars.

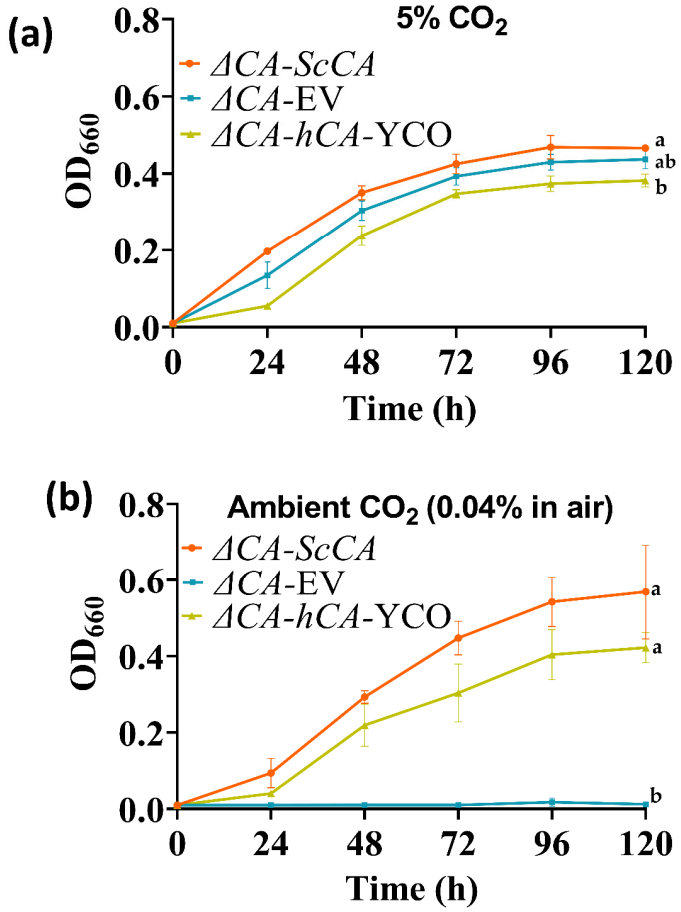

Figure 3. Δ*CA-hCA*-YCO can grow in limiting-CO_2 conditions in liquid media, similar to Δ*CA-ScCA*. Δ*CA-ScCA*, Δ*CA*-EV, and Δ*CA-hCA*-YCO cells were grown in liquid YM (-his,-trp) and incubated at 30 °C in (**a**) 5% and (**b**) ambient CO_2 for 120 h. The cultures were standardized to an initial OD_{600} of 0.01 in 50 mL. Points in the graph represent means, and error bars represent standard errors (n = 3). Statistical significance for the last time point (120 h) was computed with ANOVA and Tukey's post hoc HSD test ($p < 0.05$), and different statistical groups are represented by letters.

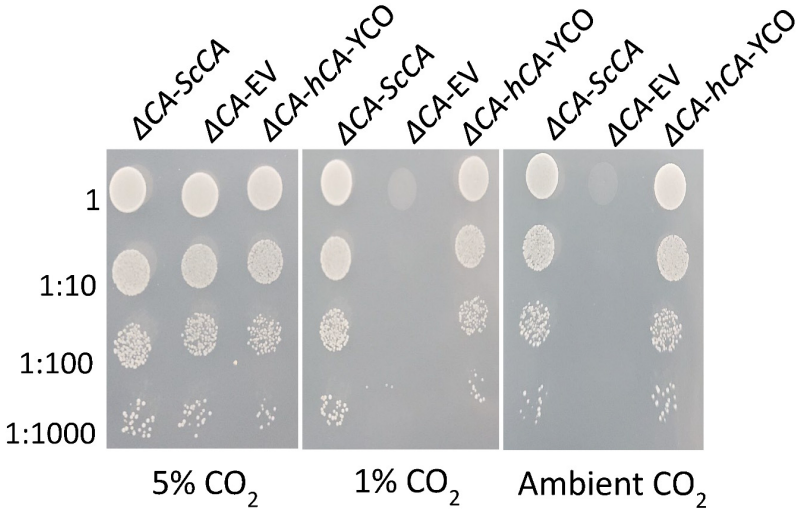

Figure 4. Δ*CA-hCA*-YCO can grow in limiting-CO_2 conditions on solid media, similar to Δ*CA*-ScCA. Δ*CA-ScCA*, Δ*CA*-EV, and Δ*CA-hCA*-YCO cells were grown to logarithmic phase then plated in 10 µL spots on YM (-his,-trp) plates and incubated at 30 °C in 5%, 1%, and ambient (0.04%) CO_2 for 3 days. The cells were standardized to an initial OD_{600} of 0.1 and serially diluted before plating.

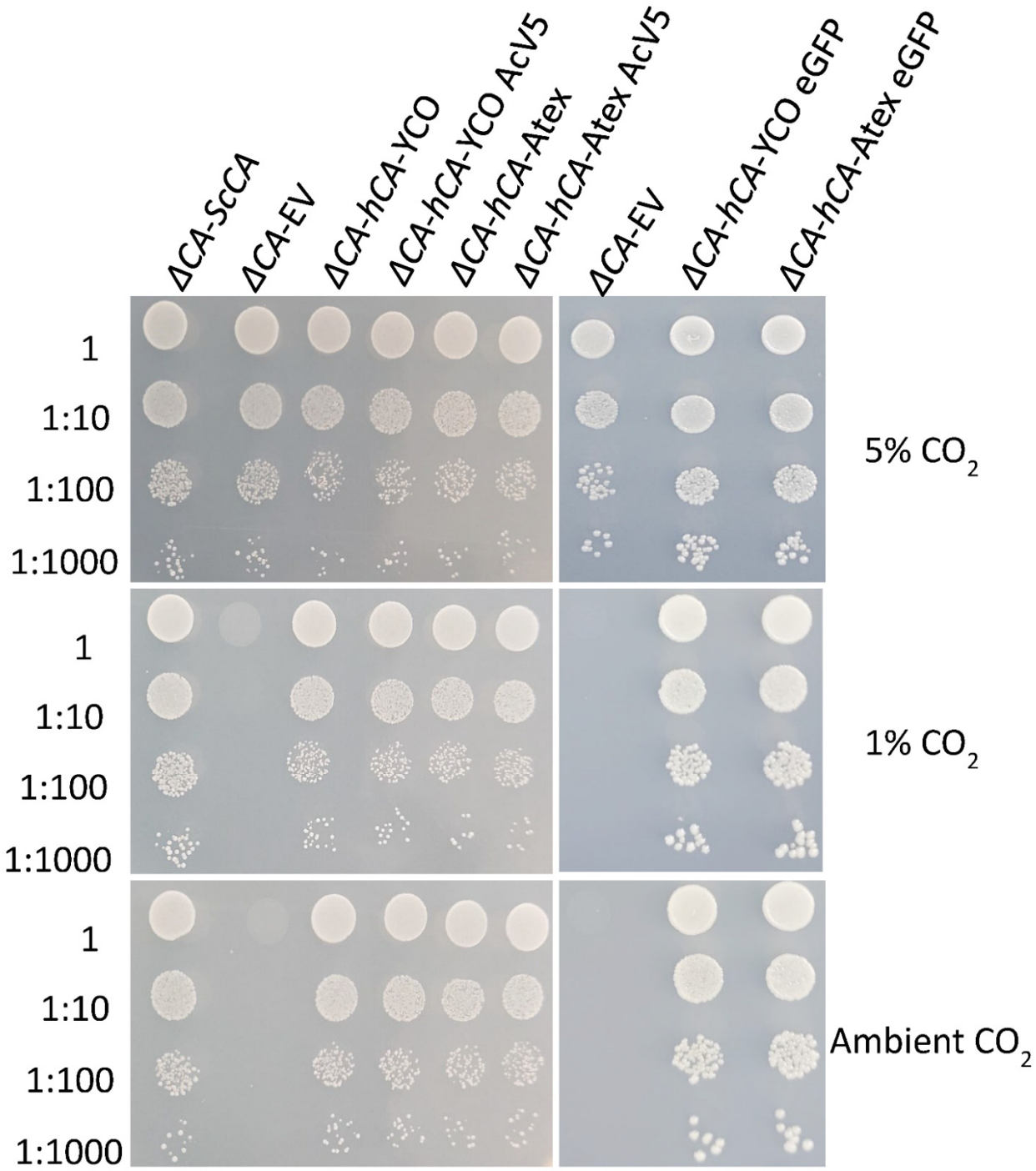

Figure 5. Δ*CA* complemented with modified *hCAs* can grow in limiting-CO_2 conditions. Modified Δ*CA*-*hCA* constructs still grow in limiting-CO_2 conditions regardless of codon optimization or added tags. Δ*CA*-*ScCA*, Δ*CA*-EV, Δ*CA*-*hCA*-YCO, Δ*CA*-*hCA*-YCO AcV5, Δ*CA*-*hCA*-YCO eGFP, Δ*CA*-*hCA*-Atex, Δ*CA*-*hCA*-Atex AcV5, and Δ*CA*-*hCA*-Atex eGFP cells were grown to logarithmic phase then plated in 10 µL spots on YM (-his,-trp) plates and incubated at 30 °C in 5%, 1%, and ambient (0.04%) CO_2 for 3 days. The cells were standardized to an initial OD_{600} of 0.1 and serially diluted before plating.

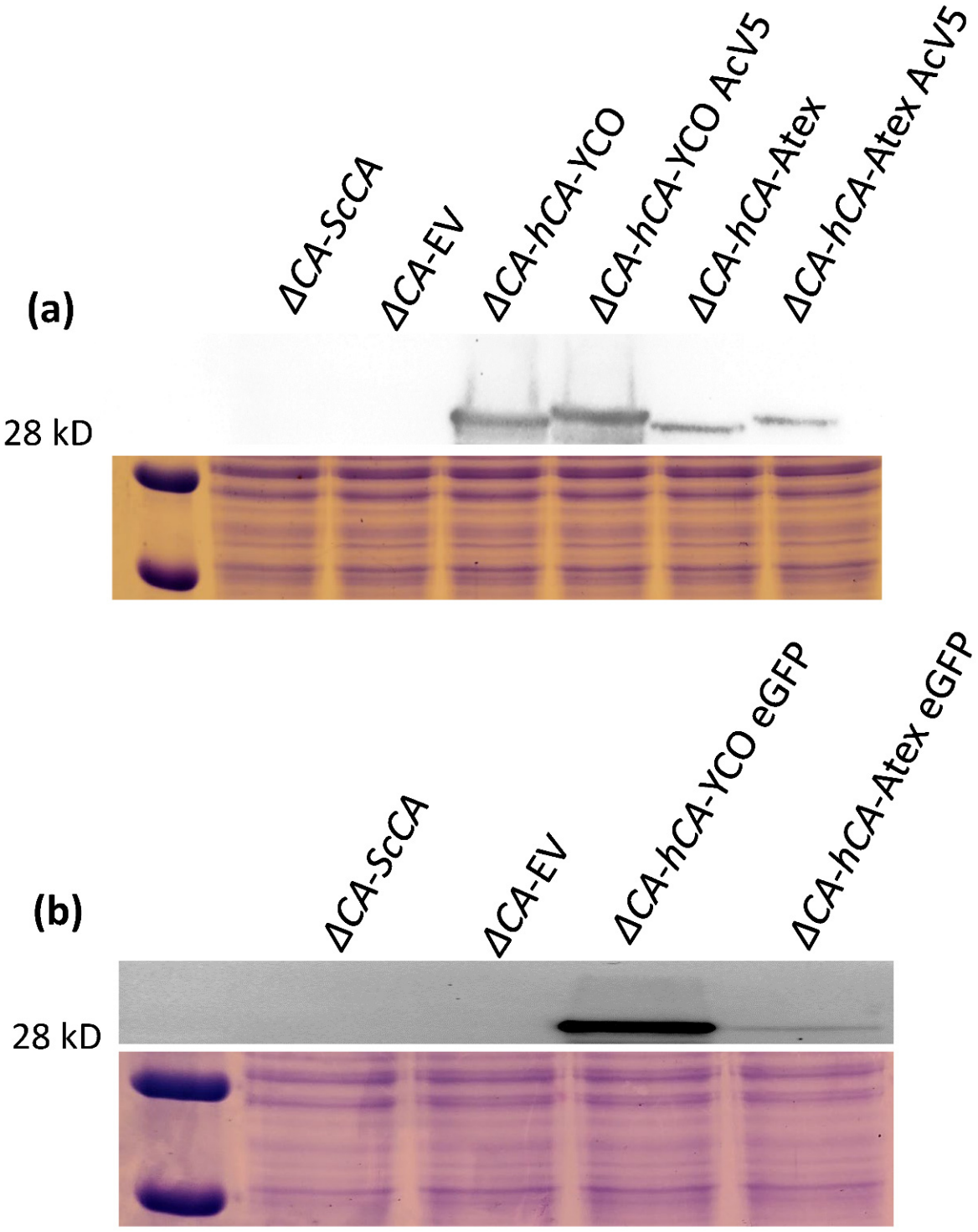

Figure 6. Immunological detection of modified hCAs in Δ*CA*. (**a**) Immunoblot showing hCA expression in Δ*CA-ScCA*, Δ*CA*-EV, Δ*CA-hCA*-YCO, Δ*CA-hCA*-YCO AcV5, Δ*CA-hCA*-Atex, and Δ*CA-hCA*-Atex AcV5. (**b**) Immunoblot showing hCA expression in Δ*CA-ScCA*, Δ*CA*-EV, Δ*CA-hCA*-YCO eGFP, and Δ*CA-hCA*-Atex eGFP. Cells were grown in liquid YM (-his,-trp) and 5% CO_2 for 72 h prior to extracting protein. Below the immunoblots are SDS-Page gels loaded with the same protein samples and stained with Coomassie Blue.

2.3. Plant and Algal Carbonic Anhydrases Show CA Activity in ΔCA-Based Heterologous Complementation System

To test the hypothesis that the Δ*CA*-based heterologous complementation system can rapidly detect the activity of different algal CA isoforms, we expressed the *C. reinhardtii* β-carbonic anhydrase CAH5 and α-carbonic anhydrase CAH3 in Δ*CA*. Expression of CAH5 restored a normal growth phenotype in the Δ*CA* mutant when cells were grown in ambient CO_2 and 1% CO_2 (Figure 7). CAH5 protein expression was detected in Δ*CA-CrCAH5* and in the positive control D66 (a wild-type *C. reinhardtii* strain) (Figure 8a). The full-length coding sequence (CDS) was used for the expression of CAH5 in Δ*CA*. The Western blot shows that *S. cerevisiae* was able to process the N-terminal mitochondrial sequence of CAH5 (Figure 8a). We observed a full-length polypeptide of 27.8 kD and a cleaved polypeptide of 20.4 kD, which is similar to the size observed in the positive control. This is the first report showing that CAH5 is an active CA in a heterologous system. The expression of CAH3 in Δ*CA-CrCAH3*-YCO restored growth in 1% CO_2, but no growth was observed in ambient CO_2 (Figure 7). In the Δ*CA-CrCAH3* strain containing the native *C. reinhardtii CAH3* gene, growth was not restored in either limiting-CO_2 condition. The Western blot shows CAH3 expression in Δ*CA-CrCAH3*-YCO and in the positive control (Figure 8b).

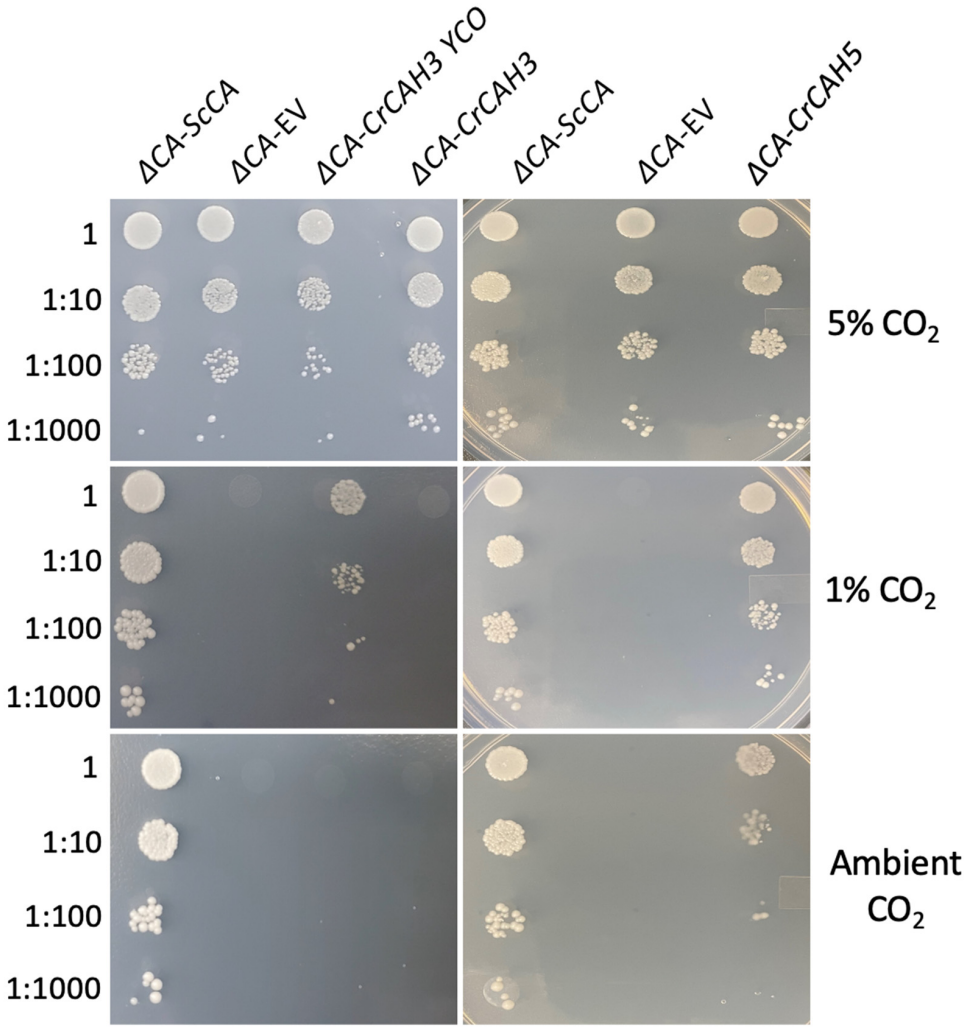

Figure 7. Δ*CA* complemented with *CrCAH3* and *CrCAH5* can grow in limiting-CO_2 conditions. Δ*CA* complemented with *CrCAH3* (YCO) can grow in 1% CO_2, while Δ*CA* complemented with *CrCAH5* can grow in 1% CO_2 and ambient CO_2. Δ*CA-ScCA*, Δ*CA*-EV, Δ*CA-CrCAH3*-YCO, Δ*CA-CrCAH3*, and Δ*CA-CrCAH5* cells were grown to logarithmic phase then plated in 10 µL spots on YM (-his,-trp) plates and incubated at 30 °C in 5% CO_2, 1% CO_2, and ambient CO_2 (0.04%) for 3 days. The cells were standardized to an initial OD_{600} of 0.1 and serially diluted before plating.

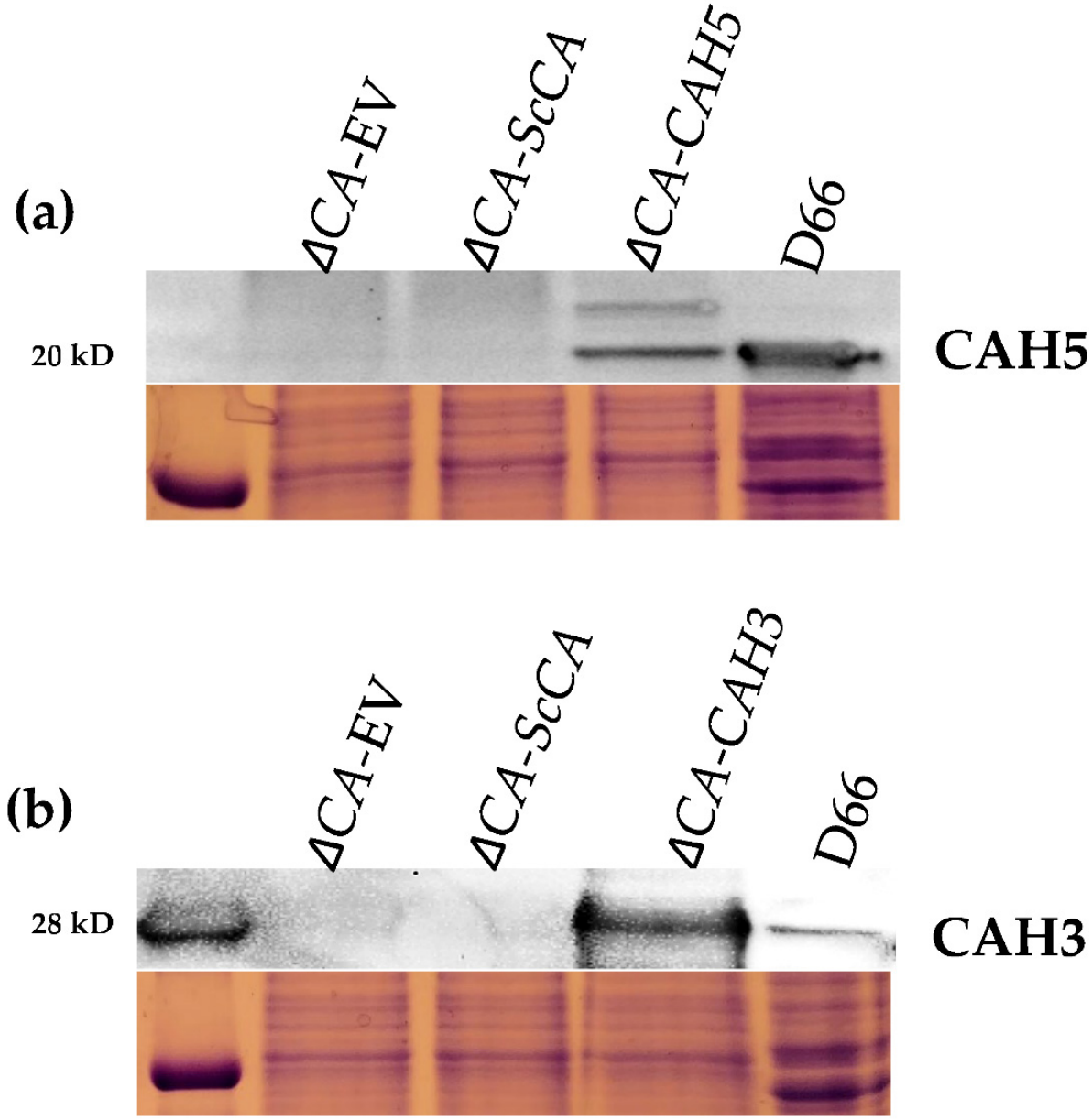

Figure 8. Immunological detection of CrCAH5 and CrCAH3 in Δ*CA*. (**a**) Immunoblot showing CrCAH5 expression in Δ*CA*-EV, Δ*CA-ScCA*, Δ*CA-CrCAH5,* and wild-type *C. reinhardtii* cells (D66). (**b**) Immunoblot showing CrCAH3 expression in Δ*CA*-EV, Δ*CA-ScCA*, Δ*CA-CrCAH3*, and wild-type *C. reinhardtii* cells (D66). *S. cerevisiae* cells were grown in liquid YM (-his,-trp) and 5% CO_2 for 72 h prior to extracting protein. *C. reinhardtii* cells were grown in MIN media and low CO_2 conditions for 12 h prior to extracting protein. Below the immunoblots are SDS-Page gels loaded with the same protein samples and stained with Coomassie Blue.

To test the activity of plant carbonic anhydrases in Δ*CA*, we transformed the *S. cerevisiae* mutant with the cytosolic carbonic anhydrase βCA3 from Arabidopsis. Normal growth was observed in Δ*CA-AtβCA3* at all three CO_2 levels (Figure 9). This result suggests that βCA3 is an active CA.

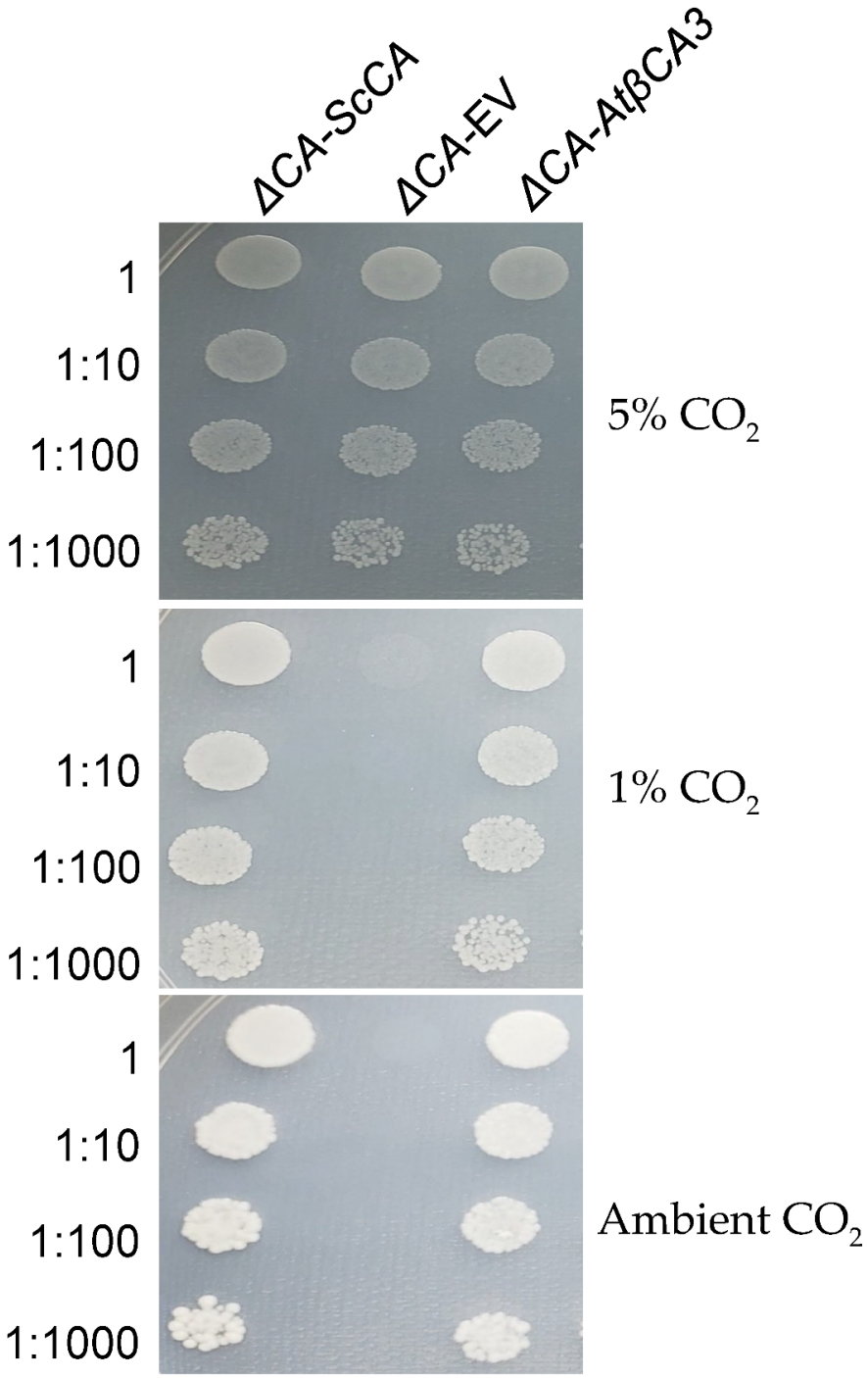

Figure 9. Δ*CA* complemented with *AtβCA3* can grow in limiting-CO_2 conditions. Δ*CA-ScCA*, Δ*CA*-EV, and Δ*CA-AtβCA3* cells were grown to logarithmic phase then plated in 10 µL spots on YM (-his,-trp) plates and incubated at 30 °C in 5% CO_2, 1% CO_2, and ambient CO_2 (0.04%) for 3 days. The cells were standardized to an initial OD_{600} of 0.01 and serially diluted before plating.

2.4. ΔCA-Based Heterologous Complementation System Can Be Used to Quantify CA Activity Using Wilbur–Anderson Assay and MIMS

To rapidly quantify the activity of normal or modified CAs in the Δ*CA* system, we used the Wilbur–Anderson assay and MIMS. The Wilbur–Anderson assay was successful in demonstrating the CA activity of Δ*CA* strains complemented with different variants of hCA (Table 1). CA activity was recorded as 4.7 ± 0.5 WAU mg^{-1} in Δ*CA-hCA*-YCO, which was the highest of all tested strains. The addition of AcV5 and eGFP decreased the

CA activity to 3.9 ± 0.4 WAU mg^{-1} and 2.5 ± 0.3 WAU mg^{-1}, respectively. In the strains using Atex genes, CA activity was further reduced. The strain Δ*CA-hCA*-Atex showed CA activity around 1.9 ± 0.2 WAU mg^{-1}. Similar to the tagged YCO strains, the addition of AcV5 and eGFP decreased CA activity to 0.9 ± 0.1 WAU mg^{-1} and 1.4 ± 0.2 WAU mg^{-1}, respectively. CA activity was also measured in the Δ*CA* strains using MIMS (Figure 10). We found that the cell lysate in Δ*CA-hCA*-YCO exhibited maximum CA activity. The AcV5 and eGFP tags reduced the CA activity significantly, consistent with measurements obtained using the Wilbur–Anderson assay.

Table 1. The Wilbur–Anderson assay can be used to measure CA activity in the Δ*CA* mutant. The Wilbur–Anderson CA assay was performed on protein extracts from Δ*CA* strains grown in 5% CO_2 for 72 h. One WAU = $(t_0 - t)/t$ where t_0 is the time for the uncatalyzed reaction and t is the time for the enzyme-catalyzed reaction. The negative control (Δ*CA*-EV) has an activity of 0.9 ± 1 WAU mg^{-1}.

Biochemical Trait	Δ*CA-hCA*-YCO	Δ*CA-hCA*-YCO AcV5	Δ*CA-hCA*-Atex	Δ*CA-hCA*-Atex AcV5	Δ*CA-hCA*-YCO eGFP	Δ*CA-hCA*-Atex eGFP	Δ*CA*-EV	Δ*CA*-ScCA
Specific activity	4.7 ± 0.5 WAU mg^{-1}	3.9 ± 0.4 WAU mg^{-1}	1.9 ± 0.2 WAU mg^{-1}	0.9 ± 0.1 WAU mg^{-1}	2.5 ± 0.3 WAU mg^{-1}	1.4 ± 0.2 WAU mg^{-1}	0.9 ± 0.1 WAU mg^{-1}	1.2 ± 0.1 WAU mg^{-1}

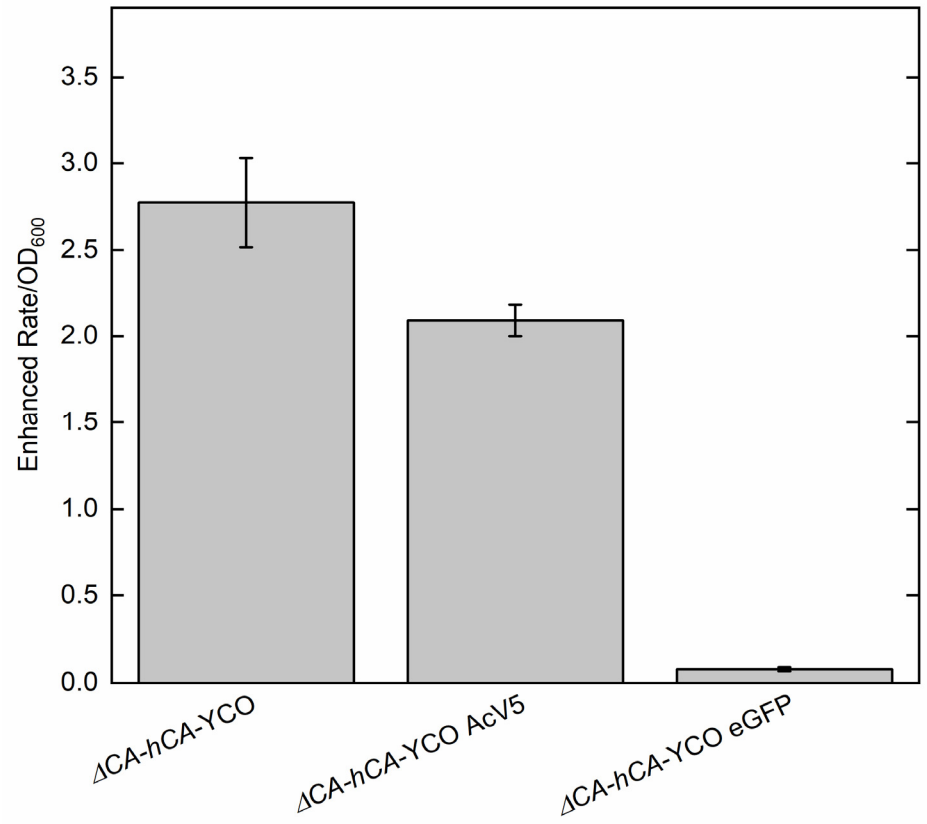

Figure 10. MIMS can be used to measure CA activity in Δ*CA* strains. MIMS assays were performed at 25 °C and pH 7.4 on protein extracts from Δ*CA-hCA*-YCO, Δ*CA-hCA*-YCO AcV5, and Δ*CA-hCA*-YCO eGFP. All strains were grown in ambient CO_2 for 48 h. The enhanced rate of ^{18}O exchange between $^{13}C^{18}O_2$ and $H_2{}^{16}O$ was calculated as the ratio between the catalyzed rate of ^{18}O loss from $^{13}C^{18}O_2$ and the uncatalyzed rate in the absence of CA. Columns and error bars represent the mean ± standard deviation of three technical replicates for each *S. cerevisiae* strain.

3. Discussion

In this report, an *S. cerevisiae* CA knock-out strain (Δ*NCE103* or Δ*CA*) was utilized as a successful heterologous system for screening active carbonic anhydrases from plants and algae. Additionally, Δ*CA* has previously been reported as a potential tool for accelerating

the discovery of non-sulfonamide-based CAIs (carbonic anhydrase inhibitors) for the treatment of CA-related diseases, such as glaucoma [30].

In this study, Δ*CA* was generated and found to have a high-CO_2-dependent phenotype, meaning it requires high-CO_2 conditions to survive (Figure 1). This clear high CO_2 growth requirement indicates that Δ*CA* strains can be used for fast and accurate screening of CA activity or active bicarbonate transport. To confirm this hypothesis, we tested CAs from human red blood cells (hCA), Arabidopsis, and *C. reinhardtii* in the heterologous *S. cerevisiae* system. Along with rapidly screening for CA activity, Δ*CA* can also be used for the estimation of CA enzymatic activity using the Wilbur–Anderson assay and MIMS.

In mammals, CAs are expressed in almost all tissues and are involved in oxygen transport between lungs, red blood cells and tissues; pH regulation; ion exchange in the kidney; and electrical activity in the retina and nervous system [31–33]. Autotrophic organisms use CAs in CCMs, where CAs are involved in increasing inorganic carbon for carbon fixation [3]. In contrast, very little is known about the physiological role of CAs in heterotrophic microbes. According to Aguilera et al. [18], the CA-deficient *S. cerevisiae* mutant's need for elevated CO_2 concentrations originates from three bicarbonate-dependent carboxylation reactions catalyzed by pyruvate decarboxylase, acetyl-CoA carboxylase, and carbamoyl phosphate synthetase. These enzymes are involved in the synthesis of C_4 intermediates, fatty acids, arginine, and uracil, respectively [34]. These observations demonstrate that the *S. cerevisiae* CA is a key biosynthetic enzyme responsible for the viability of *S. cerevisiae* under aerobic conditions. Since Δ*CA* was complemented at air levels of CO_2 by the addition of hCA (Figures 3 and 4), we investigated whether fatty acid biosynthesis is bicarbonate-dependent at air levels of CO_2 (Figure 2). *S. cerevisiae* uses acetyl-CoA as a building block to synthesize neutral lipids (NL) such as triglycerides (TGs) and sterol-esters (SEs). Acetyl-CoA is first converted into malonyl-CoA by acetyl-CoA carboxylase, using HCO_3^- as a substrate. *S. cerevisiae* cells deficient in acetyl-CoA carboxylase are not able to make long chain saturated fatty acids for de novo growth [35]. To test our hypothesis, we introduced ^{14}C-acetic acid to Δ*CA-ScCA*, Δ*CA*-EV, and Δ*CA-hCA* grown on air levels of CO_2 for one hour. Acetic acid is rapidly converted into acetyl-CoA by acetyl-CoA synthetase (ACS2), which makes ^{14}C-acetic acid, a suitable radiolabeling substrate in *S. cerevisiae*. We observed that radiolabeled ^{14}C is incorporated into the chloroform–methanol fraction containing NLs. The incorporation of radiolabeled ^{14}C into NLs occurs at a higher count in Δ*CA-hCA* than in Δ*CA-ScCA* and Δ*CA*-EV (Figure 2). This result confirmed that CAs produce HCO_3^- for the NL biosynthesis pathway. However, there are other bicarbonate-requiring pathways that are also involved in limiting the growth of Δ*CA* in air. Hence, if we introduce CAs or HCO_3^- transporters from plants and algae, they can help to increase the HCO_3^- pool required for different biological processes in the cell. This makes the Δ*CA* heterologous complementation system useful for identifying new bicarbonate transporters or CAs as suitable candidates to improve photosynthetic efficiency in C_3 crop plants.

This report shows that hCA displayed sufficient CA activity to rescue Δ*CA* grown on air levels of CO_2 (Figures 3 and 4). The results extend the work of Sangkaew et al. [30] who used this Δ*CA* system to screen CA inhibitors. To test modified CAs, *S. cerevisiae* codon-optimized (YCO) and Arabidopsis codon-optimized (Atex) hCA genes with added eGFP and AcV5 tags were used to complement Δ*CA* (Figure 5. The hCA protein was detected in all the hCA variants, but the amount of protein was highest in *S. cerevisiae* codon-optimized hCA (Figure 6a,b). The different variants of hCA complement Δ*CA* even though the protein content differs in the strains. This relates to the concept that only a low amount of CA activity is needed to maintain vital biological functions in *S. cerevisiae* since CA is such a fast enzyme. This concept is also supported by plant studies showing that the majority of CA activity within the plant needs to be removed in order to observe a growth phenotype [10]. Although all the hCA variants rescued Δ*CA*, CA activity was highest in the strain using *S. cerevisiae* codon-optimized hCA (Table 1 and Figure 10). The low CA activity in Atex strains might also be because of low protein expression (Figure 6a,b). In terms of the effect of added tags, the MIMS and Wilbur–Anderson assay

data showed that the addition of longer tags resulted in a larger reduction in CA activity. The hCA tagged with eGFP has lower CA activity compared to the hCA tagged with AcV5 (Table 1 and Figure 10). These results suggest that the Δ*CA* system can be used to rapidly test the suitability of carbonic anhydrases before introducing them into C_3 plants. Tags such as eGFP and AcV5 are widely used to determine the subcellular location of CAs, but there is a possibility that these tags can affect the functionality of the proteins. Thus, the Δ*CA*-based heterologous complementation system provides a rapid pipeline for the systematic assessment of normal and modified CAs before introducing them into C_3 plants. Mathematical models predict that installing a CCM into C_3 plants could improve leaf CO_2 uptake by up to 60% [36,37]. Hence, using Δ*CA* in conjugation with the Wilbur–Anderson assay and MIMS can shorten the process of selecting suitable CCM components from cyanobacteria and algae to transform into terrestrial C_3 plants.

To check the CA activity from an algal system, we expressed the β-carbonic anhydrase, CAH5, and the α-carbonic anhydrase, CAH3, from *C. reinhardtii* in Δ*CA*. CAH5 is present in the mitochondrial matrix and is required to maintain optimal rates of photoautotrophic growth on ambient levels of CO_2 [25]. CAH5 restores the growth of Δ*CA* at air levels of CO_2 and 1% CO_2, but the rescued phenotype is weak compared to Δ*CA*-*ScCA* (Figure 7). This might indicate that CAH5 is a low-activity CA. Mitochondrial CA in *C. reinhardtii* is encoded by two genes (*CAH4* and *CAH5*). This genetic redundancy could help the cell increase the amount of CA in the mitochondria since the enzyme has low activity, but it seems wasteful to produce large amounts of a protein with low activity rather than making a protein with high activity. The α carbonic anhydrase CAH3 was also tested in Δ*CA*. It is located in the thylakoid lumen in *C. reinhardtii* and has also been identified as an important component to maintain the CCM at low CO_2 levels [38,39]. It was previously reported that CrCAH3 is different from other α carbonic anhydrases given that it has an optimum CA activity at lower pH values than CAs of the same type, which normally operate at pH 7.0 and higher [6,40]. *S. cerevisiae* codon-optimized CAH3 restored the normal growth phenotype in Δ*CA* at 1% CO_2 but not at air levels, indicating that CAH3 activity might have been reduced because the *S. cerevisiae* cytoplasmic pH is around 7 (Figure 7). The Western blot clearly shows that CrCAH3 is produced in Δ*CA* (Figure 8b). The chloroplast transit peptide was removed from CrCAH3. The low activity could also be attributed to our use of a truncated version of CAH3 in Δ*CA*, although the protein length we used was reported to be the mature protein size [6,26]. Another possibility is that CAH3 requires post-translational modifications. Blanco-Rivero, et al. [41] reported that kinase activity is needed to activate CAH3 inside the lumen. The complementation of CrCAH5 and CrCAH3 (both YCO) in Δ*CA* suggests that the Δ*CA*-based heterologous complementation system can detect active CA enzymes from algal systems.

In general, α-carbonic anhydrases are structurally simpler than β-carbonic anhydrases and often have high specific activity. Humans only have α-carbonic anhydrases, while plants and algae have a wide variety of carbonic anhydrase families from α, β, γ, and θ classes. These CAs are localized to different intercellular and intracellular locations. Hence, the Δ*CA* heterologous complementation system could also be used as a tool to differentiate activity between CA families, which could help researchers select better CA candidates to integrate into C_3 crop plants.

To check if Δ*CA* is rescued by a plant's CA, we used β carbonic anhydrase βCA3, which localizes in the cytosol of Arabidopsis. βCA3 rescued Δ*CA* on 1% CO_2 and air levels of CO_2, showing that it is an active CA enzyme (Figure 9).

After transforming crop plants with a protein, the main challenge occurs upon trying to determine if the protein is functional once it is correctly localized. The addition of a fluorescent tag reveals if the protein is in the correct location, but it cannot report if the protein is in the correct orientation in the membrane or if it is functional. In addition, when GFP is added to a protein, the protein is modified because an entire second protein has been attached. This modification could potentially alter the CAs' activity. The heterologous Δ*CA*-based system is an important tool for rapidly checking the activity of normal or

modified CAs before integrating them into C_3 crop plants to improve photosynthetic efficiency (Figure 11a,b). The Δ*CA* system can also check the activity of proteins retargeted to different compartments in plants.

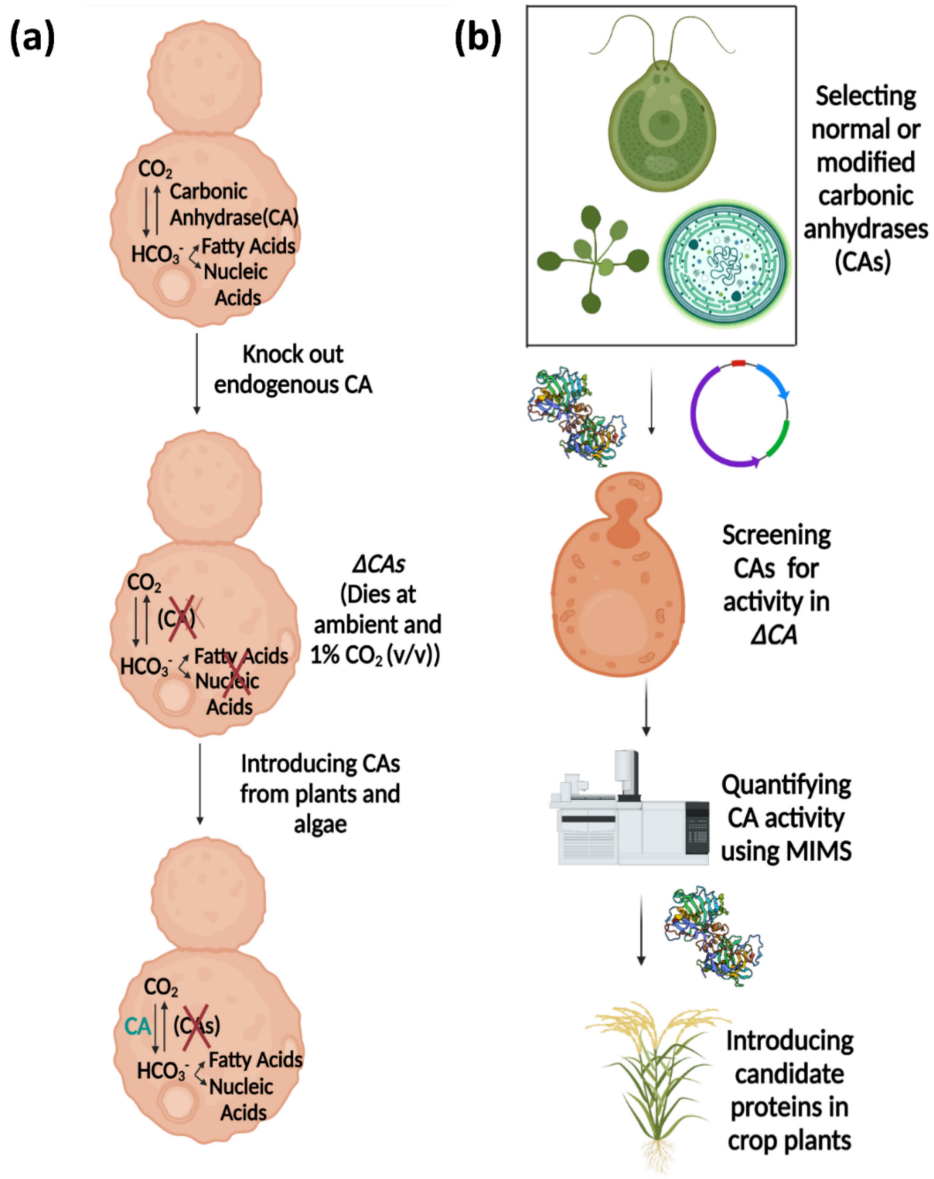

Figure 11. Model proposing the use of Δ*CA*-based heterologous complementation systems to detect CA activity. In (**a**) the importance of carbonic anhydrase (CA) for the growth of *S. cerevisiae* at ambient CO_2 is shown and (**b**) discusses the pipeline to use Δ*CA* as a useful tool for rapidly detecting CA activity before introducing normal or modified CAs in crop plants.

4. Materials and Methods

4.1. S. cerevisiae Strain and Growth Conditions

Saccharomyces cerevisiae strain DDY2 (*S. cerevisiae* W303-1a diploid variant) was used as the starting stock for the generation of a CA knock-out (Δ*NCE103*). Yeast minimal media (YM) supplemented with 6.7 g/L yeast nitrogen base, 20% (*w*/*v*) dextrose, and an amino acid mix was used to grow liquid cultures of the *S. cerevisiae* cells. YM plates were made by adding 1.5% (*w*/*v*) agar to liquid YM. The Δ*CA* generated in this study was grown in 5% (*v*/*v*) CO_2 in air at 30 °C, unless otherwise stated. Liquid cultures were grown on a rotary shaker at 30 °C in 5% (*v*/*v*) CO_2 in air and ambient CO_2 (0.04% (*v*/*v*) CO_2 in air). *S. cerevisiae* cells were grown on YM plates in three different CO_2 conditions: 5% (*v*/*v*)

CO_2 in the air, 1% (v/v) CO_2 in the air, and ambient CO_2 (0.04% (v/v) CO_2 in the air) at 30 °C. Where applicable, amino acid mixes were added in the following order for the strains generated in this report: amino acid mix made without tryptophan (Δ*CA*), amino acid mix made without histidine and tryptophan (Δ*CA*-EV, Δ*CA*-*ScCA*, Δ*CA*-*hCA*-YCO, Δ*CA*-*hCA*-YCO AcV5, Δ*CA*-*hCA*-Atex, Δ*CA*-*hCA*-Atex AcV5, Δ*CA*-*CrCAH5*, Δ*CA*-*CrCAH3*-YCO, Δ*CA*-*CrCAH3*, and Δ*CA*-*AtβCA3*) and amino acid mix made without uracil and tryptophan (Δ*CA*-*hCA*-YCO eGFP, Δ*CA*-*hCA*-Atex eGFP).

4.2. Generation of S. cerevisiae Carbonic Anhydrase Knock-Out

The construction of the *NCE103* deletion in the diploid strain DDY2 was carried out by PCR-targeting with a *TRP1 disruption cassette* flanked by short homology regions of the *NCE103* gene [42]. The disruption cassette was obtained by amplifying the TRP1 cassette from the plasmid pRS304 ([43] and Table S1). pRS304 was used as a template in a PCR reaction to amplify TRP1 with *NCE103* flanking sequences using oligonucleotides DDO-1976 and -1977. This DNA was concentrated by ethanol precipitation and transformed into *S. cerevisiae* strain DDY2. The transformation mix was plated onto minimal media lacking tryptophan to screen for Δ*NCE103* mutants. The successful haploid knock-outs were confirmed by PCR using primers described in Table S1. Correctly targeted strains were sporulated to haploid, and Trp+ isolates were re-confirmed by PCR as Δ*NCE103* mutants.

4.3. Genetic Constructs and Vectors

To express the mature peptide versions of human CAII (HCAII; Genbank ID AK312978) and *CrCAH3*-YCO (referred to as yeast codon-optimized (YCO)) in Δ*NCE103*, the *hCA* and *CrCAH3* gene was synthesized by GenScript in pENTR and cloned into destination vectors MGO515 (-HIS) and MGO528 (-URA) using Gateway cloning. The *hCA* gene was codon optimized for *S. cerevisiae* (referred to as yeast codon-optimized (YCO)) and Arabidopsis (referred to as Arabidopsis codon-optimized (Atex)). A C-terminal AcV5 tag and eGFP tag were added to the *hCA* gene (Figure S1). *hCA* (with or without *Acv5* tag) coding sequences were commercially synthesized (Genscript) as gateway-enabled entry vectors (i.e., included flanking attL sites). A second set of *hCAII* genes without the stop codon were also made, for use in GFP C-terminal fusion constructs. The *hCAII* coding sequences (CDS) were cloned into plasmids from the Advanced Gateway® adapted pRS series of yeast expression plasmids [44] using Gateway *LR Clonase II* enzyme mix (Invitrogen™)—essentially swapping out the ccdB bacterial lethality cassette for the given *hCAII* CDS between the attR1/R2 sites (Figure S1). The yeast expression construct library was obtained through Addgene (https://www.addgene.org/) (kit #1000000011). pAG423GPD-ccdB (internally designated MG0515; HIS) was used for full-length CDS clones. pAG426GPD-ccdB-eGFP (internally designated MG0528; URA) was used for GFP fusions (i.e., *hCAII* CDS without stop codon). All *E. coli* cloning steps used One Shot™ OmniMAX™ (Peachtree Corners, GA, USA) 2 T1R Chemically Competent E. coli cells (Invitrogen). All final plasmids were sanger sequenced to confirm accuracy of the clones using Wizard® Plus SV Minipreps DNA Purification Systems (Promega, Madison, WI, USA), BigDye® sequencing chemistry (Thermofisher Scientific, Waltham, MA, USA), and ZR DNA Sequencing Clean-Up Kit (Zymo Research, Irvine, CA, USA). Internal catalogue designations for final yeast *hCAII* expression constructs were: MG0515.54: GPD-hCAII (YCO)-stop; MG0515.55: GPD-hCAII (YCO)-AcV5-stop; MG0515.56: GPD-hCAII (Atex)-stop; MG0515.57: GPD-hCAII (Atex)-AcV5-stop; MG0528.20: GPD-hCAII (YCO)-nostop-eGFP; MG0528.21: GPD-hCAII (Atex)-nostop-eGFP.

The genes *CrCAH5*, *CrCAH3*, *ScCA*, and *AtβCA3* were amplified by PCR from linebreak *C. reinhardtii* (D66) and *A. thaliana* (Col-0). The genes were cloned into the expression vector pDD506 using ClaI/XhoI sites for constitutive expression under control of the *ADH1* promoter (Figure S1). All DNA constructs were verified by DNA sequencing.

4.4. S. cerevisiae CA Knock-Out Transformation

The plasmid MG0515 containing *hCA*-YCO, *hCA*-YCO AcV5, *hCA*-Atex, *hCA*-Atex AcV5, and *CrCAH3*-YCO, the plasmid MGO528 containing hCA-YCO eGFP, and *hCA*-Atex eGFP, and the plasmid pDD506 containing *CrCAH5*, *CrCAH3*, and *AtβCA3* were transformed in *E. coli* TOP10 cells (One Shot™ TOP10 Chemically Competent *E. coli*). The plasmids were extracted from the transformed *E. coli* cultures using a GeneJET Plasmid Miniprep Kit (Thermo Scientific™) according to manufacturer's instructions. The plasmids were transformed in the Δ*NCE103* mutant using a *S. cerevisiae* transformation protocol as described by Gietz and Schiestl [45]. The positive colonies were screened by colony PCR using primers complementary to the genes (Table S1).

4.5. High-CO_2-Dependence Growth Assay

S. cerevisiae cell cultures were initiated from −80 °C glycerol stocks. The liquid cultures were grown to log phase in liquid YM in 5% CO_2 at 30 °C. The cultures were reinoculated for the growth assay and grown in 5% CO_2 and ambient CO_2. The optical density at 600 nm (OD_{600}) of the cultures was adjusted to an initial OD_{600} of 0.01. Relative growth rates were measured in liquid YM by monitoring the cultures' OD_{600} using a spectrometer (Thermo Fisher Scientific, Waltham, MA, USA). For the measurement of relative growth rates on solidified YM, the OD_{600} of the cultures was standardized to 0.01, and 10 µL of serial dilutions were spotted onto YM plates. The plates were incubated at 30 °C in 5%, 1%, and ambient CO_2 for 72 h. The plates were photographed after 72 h.

4.6. Immunological Detection of Expressed Proteins in S. cerevisiae

Membrane-enriched protein fractions of *S. cerevisiae* were prepared according to Zhang et al. [46]. Proteins from the *S. cerevisiae cell* lysate were mixed with 2× Laemmli sample buffer and β-mercaptoethanol and heated to 95 °C for ~7 min prior to resolution by SDS-PAGE on 12% (*v*/*v*) polyacrylamide gels (Mini-PROTEAN TGX, Bio-Rad Laboratories, Hercules, CA, USA). The expression of tagged proteins was detected immunochemically after transferring the proteins to a PVDF membrane. The membrane was blocked in TTBS (TBS with 0.1% (*v*/*v*) Tween) with 1% (*w*/*v*) bovine serum albumin at 4 °C overnight. The membrane was treated with monoclonal antibodies for 1 h at room temperature with the following dilutions: 1:1000 for hCA (Sigma-Aldrich, Darmstadt, Germany), 1:20,000 for CrCAH5 (Agrisera, Vännäs, Sweden) and 1:10,000 for CrCAH3 (Agrisera). The anti-CrCAH3 antibody is commercially available at Agrisera and the anti-CrCAH5 antibody was custom made by Agrisera. The membrane was treated with secondary anti-rabbit antibody (HRP conjugated from Bio-Rad) for 1 h at room temperature with the following dilutions: 1:500 for hCA (Sigma-Aldrich, Darmstadt, Germany) and 1:4000 for CrCAH5 and CrCAH3. Antibody binding was visualized by fluorescence detection with Thermo Scientific™ Pierce™ ECL Western Blotting Substrate on a Chemi-Doc XRS (Bio-Rad, Hercules, CA, USA).

4.7. Analysis of Neutral Lipid Synthesis Using Radiolabel ^{14}C-Acetic Acid

^{14}C-acetic acid was incorporated in *S. cerevisiae* using the protocol described by Rogers and Henne [22], except that 50 µL of radiolabeling media was added to 1 mL of cell suspension (final ^{14}C-acetic acid concentration = 1.25 µCi/mL). Here, a 1 h radiolabeling pulse incubation was used to label neutral lipid species in Δ*CA*, Δ*CA-ScCA* and Δ*CA-hCA*-YCO.

4.8. Carbonic Anhydrase Activity Assay

CA activity was measured by the Wilbur–Anderson assay according to Mitra et al. [47]. The isotope exchange membrane-inlet mass spectrometry (MIMS) technique was used to measure CA activity as described by Price and Badger [48]. Briefly, 20 µL of *S. cerevisiae* cell lysate was added to a temperature controlled, 2 mL reaction cuvette connected to the inlet of a Finnegan DELTA-V Isotope Ratio Mass Spectrometer (Thermo Fisher Scientific). The 2 mL CA assay consisted of 100 mM HEPES-KOH (pH 7.4), 5 mM dithiothreitol, and

$^{13}C^{18}O_2$. The enhanced rate of ^{18}O exchange between $^{13}C^{18}O_2$ and $H_2{}^{16}O$ was calculated as a ratio between the increase in ^{18}O loss from $^{13}C^{18}O_2$ in the presence of CA compared to the uncatalyzed rate. Three technical replicates were run at 25 °C for each CA enzyme tested [10].

Supplementary Materials: The following supporting information can be downloaded at: https://www.mdpi.com/article/10.3390/plants11141882/s1; Figure S1: Plasmids pDD506(HIS3), MGO515(HIS3), and MGO528(URA3) were used in this study for the overexpression of proteins in *S. cerevisiae*, Figure S2: Relative intensity of the modified hCA bands for the immunoblot experiment shown in Figure 6a,b; Table S1: Primers used in this study for cloning.

Author Contributions: A.K.R. and J.V.M. designed the research; A.K.R., M.G., R.J.D., R.W.K. and J.V.M. performed the research. All authors along with A.B.C. and D.D. provided critical feedback and helped shape the research, analysis, and manuscript. All authors have read and agreed to the published version of the manuscript.

Funding: This work was supported by the Realizing Improved Photosynthetic Efficiency (RIPE) initiative awarded to JVM by the University of Illinois, Champaign, IL, USA. RIPE is made possible through support from the Bill & Melinda Gates Foundation, FFAR, and FCDO, grant no. OPP1172157. This study was also supported in part by the Division of Chemical Sciences, Geosciences, and Biosciences, Office of Basic Energy Sciences, Department of Energy (grant no. DE-SC0001685) to A.B.C.

Institutional Review Board Statement: Not applicable.

Informed Consent Statement: Not applicable.

Data Availability Statement: All of the new data is contained within this article or the supplementary material.

Acknowledgments: The authors express their gratitude to Lillian LaPlace, Isaiah C. Pabuayon and Timothy Chen, Louisiana State University, Baton Rouge, LA, USA, for their valuable suggestions in improving the manuscript. The authors are also thankful to BioRender.com for help in creating Figure 11a,b.

Conflicts of Interest: The authors declare no conflict of interest.

References

1. Supuran, C.T. Structure and function of carbonic anhydrases. *Biochem. J.* **2016**, *473*, 2023–2032. [CrossRef] [PubMed]
2. DiMario, R.J.; Machingura, M.C.; Waldrop, G.L.; Moroney, J.V. The many types of carbonic anhydrases in photosynthetic organisms. *Plant Sci.* **2018**, *268*, 11–17. [CrossRef] [PubMed]
3. Sültemeyer, D.; Schmidt, C.; Fock, H.P. Carbonic anhydrases in higher plants and aquatic microorganisms. *Plant Physiol.* **1993**, *88*, 179–190. [CrossRef]
4. Moroney, J.V.; Ma, Y.; Frey, W.D.; Fusilier, K.A.; Pham, T.T.; Simms, T.A.; DiMario, R.J.; Yang, J.; Mukherjee, B. The carbonic anhydrase isoforms of *Chlamydomonas reinhardtii*: Intracellular location, expression, and physiological roles. *Photosynth. Res.* **2011**, *109*, 133–149. [CrossRef] [PubMed]
5. Badger, M. The roles of carbonic anhydrases in photosynthetic CO_2 concentrating mechanisms. *Photosynth. Res.* **2003**, *77*, 83. [CrossRef]
6. Karlsson, J.; Clarke, A.K.; Chen, Z.Y.; Hugghins, S.Y.; Park, Y.I.; Husic, H.D.; Moroney, J.V.; Samuelsson, G. A novel alpha-type carbonic anhydrase associated with the thylakoid membrane in *Chlamydomonas reinhardtii* is required for growth at ambient CO_2. *EMBO J.* **1998**, *17*, 1208–1216. [CrossRef]
7. Espie, G.S.; Kimber, M.S. Carboxysomes: Cyanobacterial RubisCO comes in small packages. *Photosynth. Res.* **2011**, *109*, 7–20. [CrossRef]
8. Price, G.D.; Coleman, J.R.; Badger, M.R. Association of carbonic anhydrase activity with carboxysomes isolated from the cyanobacterium Synechococcus PCC7942. *Plant Physiol.* **1992**, *100*, 784–793. [CrossRef]
9. Hatch, M.D.; Burnell, J.N. Carbonic Anhydrase Activity in Leaves and Its Role in the First Step of C_4 Photosynthesis. *Plant Physiol.* **1990**, *93*, 825–828. [CrossRef]
10. DiMario, R.J.; Giuliani, R.; Ubierna, N.; Slack, A.D.; Cousins, A.B.; Studer, A.J. Lack of leaf carbonic anhydrase activity eliminates the C_4 carbon-concentrating mechanism requiring direct diffusion of CO_2 into bundle sheath cells. *Plant Cell Environ.* **2022**, *45*, 1382–1397. [CrossRef]

11. DiMario, R.J.; Quebedeaux, J.C.; Longstreth, D.J.; Dassanayake, M.; Hartman, M.M.; Moroney, J.V. The Cytoplasmic Carbonic Anhydrases βCA2 and βCA4 Are Required for Optimal Plant Growth at Low CO_2. *Plant Physiol.* **2016**, *171*, 280–293. [CrossRef] [PubMed]
12. Medina-Puche, L.; Castelló, M.J.; Canet, J.V.; Lamilla, J.; Colombo, M.L.; Tornero, P. β-carbonic anhydrases play a role in salicylic acid perception in Arabidopsis. *PLoS ONE* **2017**, *12*, e0181820. [CrossRef] [PubMed]
13. Hines, K.M.; Chaudhari, V.; Edgeworth, K.N.; Owens, T.G.; Hanson, M.R. Absence of carbonic anhydrase in chloroplasts affects C_3 plant development but not photosynthesis. *Proc. Natl. Acad. Sci. USA* **2021**, *118*, e2107425118. [CrossRef]
14. Atkinson, N.; Mao, Y.; Chan, K.X.; McCormick, A.J. Condensation of Rubisco into a proto-pyrenoid in higher plant chloroplasts. *Nat. Commun.* **2020**, *11*, 6303. [CrossRef] [PubMed]
15. Hennacy, J.H.; Jonikas, M.C. Prospects for engineering biophysical CO_2 concentrating mechanisms into land plants to enhance yields. *Annu. Rev. Plant Biol.* **2020**, *71*, 461–485. [CrossRef]
16. Long, B.M.; Hee, W.Y.; Sharwood, R.E.; Rae, B.D.; Kaines, S.; Lim, Y.-L.; Nguyen, N.D.; Massey, B.; Bala, S.; von Caemmerer, S.; et al. Carboxysome encapsulation of the CO_2-fixing enzyme Rubisco in tobacco chloroplasts. *Nat. Commun.* **2018**, *9*, 3570. [CrossRef]
17. Amoroso, G.; Morell-Avrahov, L.; Müller, D.; Klug, K.; Sültemeyer, D. The gene NCE103 (YNL036w) from *Saccharomyces cerevisiae* encodes a functional carbonic anhydrase and its transcription is regulated by the concentration of inorganic carbon in the medium. *Mol. Microbiol.* **2005**, *56*, 549–558. [CrossRef]
18. Aguilera, J.; Van Dijken, J.P.; De Winde, J.H.; Pronk, J.T. Carbonic anhydrase (Nce103p): An essential biosynthetic enzyme for growth of *Saccharomyces cerevisiae* at atmospheric carbon dioxide pressure. *Biochem. J.* **2005**, *391*, 311–316. [CrossRef]
19. Whitney, P.A.; Cooper, T.G. Urea Carboxylase and Allophanate Hydrolase: Two components of adenosine triphosphate:urea amido-lyase in *Saccharomyces cerevisisae*. *J. Biol. Chem.* **1972**, *247*, 1349–1353. [CrossRef]
20. Mishina, M.; Rogguenkamp, R.; Schweizer, E. Yeast mutants defective in acetyl-coenzyme A carboxylase and biotin: Apocarboxylase ligase. *Eur. J. Biochem.* **1980**, *111*, 79–87. [CrossRef]
21. Magnuson, K.; Jackowski, S.; Rock, C.O.; Cronan, J.E. Regulation of fatty acid biosynthesis in *Escherichia coli*. *Microbiol. Rev.* **1993**, *57*, 522–542. [CrossRef] [PubMed]
22. Rogers, S.; Henne, W.M. Analysis of Neutral Lipid Synthesis in *Saccharomyces cerevisiae* by Metabolic Labeling and Thin Layer Chromatography. *J. Vis. Exp.* **2021**, *168*, e62201. [CrossRef] [PubMed]
23. Eriksson, M.; Karlsson, J.; Ramazanov, Z.; Gardeström, P.; Samuelsson, G. Discovery of an algal mitochondrial carbonic anhydrase: Molecular cloning and characterization of a low-CO_2-induced polypeptide in *Chlamydomonas reinhardtii*. *Proc. Natl. Acad. Sci. USA* **1996**, *93*, 12031–12034. [CrossRef] [PubMed]
24. Fang, W.; Si, Y.; Douglass, S.; Casero, D.; Merchant, S.S.; Pellegrini, M.; Ladunga, I.; Liu, P.; Spalding, M.H. Transcriptome-wide changes in Chlamydomonas reinhardtii gene expression regulated by carbon dioxide and the CO_2-concentrating mechanism regulator CIA5/CCM1. *Plant Cell* **2012**, *24*, 1876–1893. [CrossRef] [PubMed]
25. Rai, A.K.; Chen, T.; Moroney, J.V. Mitochondrial carbonic anhydrases are needed for optimal photosynthesis at low CO_2 levels in Chlamydomonas. *Plant Physiol.* **2021**, *187*, 1387–1398. [CrossRef] [PubMed]
26. Hanson, D.T.; Franklin, L.A.; Samuelsson, G.; Badger, M.R. The *Chlamydomonas reinhardtii cia3* mutant lacking a thylakoid lumen-localized carbonic anhydrase is limited by CO_2 supply to Rubisco and not photosystem II function in vivo. *Plant Physiol.* **2003**, *132*, 2267–2275. [CrossRef]
27. Park, Y.-I.; Karlsson, J.; Rojdestvenski, I.; Pronina, N.; Klimov, V.; Öquist, G.; Samuelsson, G. Role of a novel photosystem II-associated carbonic anhydrase in photosynthetic carbon assimilation in *Chlamydomonas reinhardtii*. *FEBS Lett.* **1999**, *444*, 102–105. [CrossRef]
28. Wilbur, K.M.; Anderson, N.G. Electrometric and colorimetric determination of carbonic anhydrase. *J. Biol. Chem.* **1948**, *176*, 147–154. [CrossRef]
29. Clark, D.; Rowlett, R.S.; Coleman, J.R.; Klessig, D.F. Complementation of the yeast deletion mutant DeltaNCE103 by members of the beta class of carbonic anhydrases is dependent on carbonic anhydrase activity rather than on antioxidant activity. *Biochem. J.* **2004**, *379*, 609–615. [CrossRef]
30. Sangkaew, A.; Krungkrai, J.; Yompakdee, C. Development of a high throughput yeast-based screening assay for human carbonic anhydrase isozyme II inhibitors. *AMB Express* **2018**, *8*, 124. [CrossRef]
31. Dodgson, S.J.; Forster, R.E.; Schwed, D.A.; Storey, B.T. Contribution of matrix carbonic anhydrase to citrulline synthesis in isolated guinea pig liver mitochondria. *J. Biol. Chem.* **1983**, *258*, 7696–7701. [CrossRef]
32. Hazen, S.A.; Waheed, A.; Sly, W.S.; Lanoue, K.F.; Lynch, C.J. Differentiation-dependent expression of CA V and the role of carbonic anhydrase isozymes in pyruvate carboxylation in adipocytes. *FASEB J.* **1996**, *10*, 481–490. [CrossRef]
33. Nocentini, A.; Donald. W., A.; Supuran, C.T. Human carbonic anhydrases: Tissue distribution, physiological role, and druggability. In *Carbonic Anhydrases*; Academic Press: Cambridge, MA, USA, 2019; pp. 151–185.
34. Lacroute, F.; Piérard, A.; Grenson, M.; Wiame, J.M. The biosynthesis of carbamoyl phosphate in *Saccharomyces cerevisiae*. *Microbiology* **1965**, *40*, 127–142.
35. Roggenkamp, R.; Numa, S.; Schweizer, E. Fatty acid-requiring mutant of *Saccharomyces cerevisiae* defective in acetyl-CoA carboxylase. *Proc. Natl. Acad. Sci. USA* **1980**, *77*, 1814–1817. [CrossRef] [PubMed]

36. Long, S.P.; Marshall-Colon, A.; Zhu, X.G. Meeting the global food demand of the future by engineering crop photosynthesis and yield potential. *Cell* **2015**, *161*, 56–66. [CrossRef] [PubMed]
37. McGrath, J.M.; Long, S.P. Can the cyanobacterial carbon-concentrating mechanism increase photosynthesis in crop species? A Theoretical Analysis. *Plant Physiol.* **2014**, *164*, 2247–2261. [CrossRef]
38. Moroney, J.V.; Tolbert, N.E.; Sears, B.B. Complementation analysis of the inorganic carbon concentrating mechanism of *Chlamydomonas reinhardtii*. *Mol. Gen. Genet. MGG* **1986**, *204*, 199–203. [CrossRef]
39. Spalding, M.H.; Spreitzer, R.J.; Ogren, W.L. Reduced inorganic carbon transport in a CO_2-requiring mutant of *Chlamydomonas reinhardii*. *Plant Physiol.* **1983**, *73*, 273–276. [CrossRef]
40. Benlloch, R.; Shevela, D.; Hainzl, T.; Grundström, C.; Shutova, T.; Messinger, J.; Samuelsson, G.; Sauer-Eriksson, A.E. Crystal structure and functional characterization of photosystem II-associated carbonic anhydrase CAH3 in *Chlamydomonas reinhardtii*. *Plant Physiol.* **2015**, *167*, 950–962. [CrossRef]
41. Blanco-Rivero, A.; Shutova, T.; Román, M.J.; Villarejo, A.; Martinez, F. Phosphorylation controls the localization and activation of the lumenal carbonic anhydrase in *Chlamydomonas reinhardtii*. *PLoS ONE* **2012**, *7*, e49063. [CrossRef]
42. Gueldener, U.; Heinisch, J.; Koehler, G.J.; Voss, D.; Hegemann, J.H. A second set of loxP marker cassettes for Cre-mediated multiple gene knockouts in budding yeast. *Nucleic Acids Res.* **2011**, *30*, e23. [CrossRef] [PubMed]
43. Sikorski, R.S.; Hieter, P. A system of shuttle vectors and yeast host strains designed for efficient manipulation of DNA in Saccharomyces cerevisiae. *Genetics* **1989**, *122*, 19–27. [CrossRef] [PubMed]
44. Alberti, S.; Gitler, A.D.; Lindquist, S. A suite of Gateway® cloning vectors for high-throughput genetic analysis in Saccharomyces cerevisiae. *Yeast* **2007**, *24*, 913–919. [CrossRef] [PubMed]
45. Gietz, R.D.; Schiestl, R.H. Frozen competent yeast cells that can be transformed with high efficiency using the LiAc/SS carrier DNA/PEG method. *Nat. Protoc.* **2007**, *2*, 1–4. [CrossRef] [PubMed]
46. Zhang, T.; Lei, J.; Yang, H.; Xu, K.; Wang, R.; Zhang, Z. An improved method for whole protein extraction from yeast *Saccharomyces cerevisiae*. *Yeast* **2011**, *28*, 795–798. [CrossRef]
47. Mitra, M.; Lato, S.M.; Ynalvez, R.A.; Xiao, Y.; Moroney, J.V. Identification of a new chloroplast carbonic anhydrase in *Chlamydomonas reinhardtii*. *Plant Physiol.* **2004**, *135*, 173–182. [CrossRef]
48. Price, G.D.; Badger, M.R. Expression of human carbonic anhydrase in the canobacterium Synechococcus PCC7942 creates a high CO_2-requiring phenotype: Evidence for a central role for carboxysomes in the CO_2 concentrating mechanism. *Plant Physiol.* **1989**, *91*, 505–513. [CrossRef]